NANO LETTERS

2005
Vol. 5, No. 3
491−495

In-situ Observation of Switchable Nanoscale Topography for Y-Shaped Binary Brushes in Fluids

Yen-Hsi Lin, Jing Teng, Eugene R. Zubarev, Hennady Shulha, and Vladimir V. Tsukruk*

Department of Materials Science and Engineering, Iowa State University, Ames, Iowa 50011

Received December 17, 2004; Revised Manuscript Received January 31, 2005

ABSTRACT

Direct, in-fluid observation of the surface morphology and nanomechanical properties of the mixed brushes composed of Y-shaped binary molecules PS–PAA revealed nanoscale network-like surface topography formed by coexisting stretched soluble PAA arms and collapsed insoluble PS chains in water. Placement of Y-shaped brushes in different fluids resulted in dramatic reorganization ranging from soft repellent layer covered by swollen PS arms in toluene to an adhesive, mixed layer composed of coexisting swollen PAA and collapsed PS arms in water. These binary layers with the overall nanoscale thickness can serve as adaptive nanocoatings with stimuli-responsive properties.

Nanoscale switchable surfaces bring a new dimension in adaptive, stimuli responsive devices and sensors. Responsive organic and polymer layers hold great promise in designing of microelectromechanical and micro-nanofluidic systems with adaptive elastic, adhesive, and adsorbing surface properties.[1−5] The macroscopic response of such "smart" surfaces controls the physical properties important in colloid stabilization, chemical gating, bioadsorption, and for tuning nanotribological behavior.[6−10] Surface composition and, hence, the surface energy, friction, elasticity, and wettability can be tailored in a completely reversible manner. Indeed, switching of surface properties has been recently observed for mixed, binary brushes grafted to a solid substrate.[11−18] However, the theoretical predictions that such brushes should form a variety of nanoscale patterns and surface micellar structures controlled by chemical attachment, grafting density, and composition has not been confirmed experimentally.[19,20]

Recently, we have introduced a novel type of Y-shaped amphiphilic brushes combining two dissimilar, hydrophobic and hydrophilic polymer chains (polystyrene (PS) and poly(acrylic acid) (PAA)) attached to a single focal point grafted to a silicon surface (Figure 1).[21] Our initial results pointed to intriguing surface properties and unusual surface nanostructures with outstanding switching ability under alternating treatments with different solvents.[22,23] However, all studies reported for these Y-shaped brushes as well as traditional mixed brushes[24] and other types of Y-shaped brushes[25] have been conducted for post-treated, dry surface layers in the

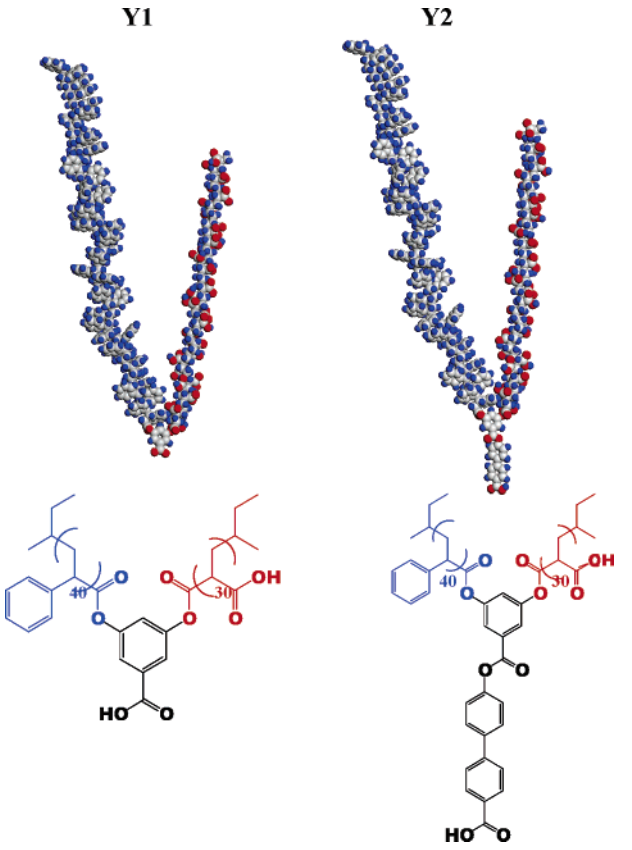

Figure 1. Chemical structure and molecular graphics representation of Y-shaped block copolymers with short (**Y1**) and long (**Y2**) aromatic functional stems. Molecules contain 40 and 30 monomeric units in PS and PAA arms, respectively.

* Corresponding author. E-mail: vladimir@iastate.edu.

10.1021/nl0479029 CCC: $30.25
Published on Web 02/15/2005

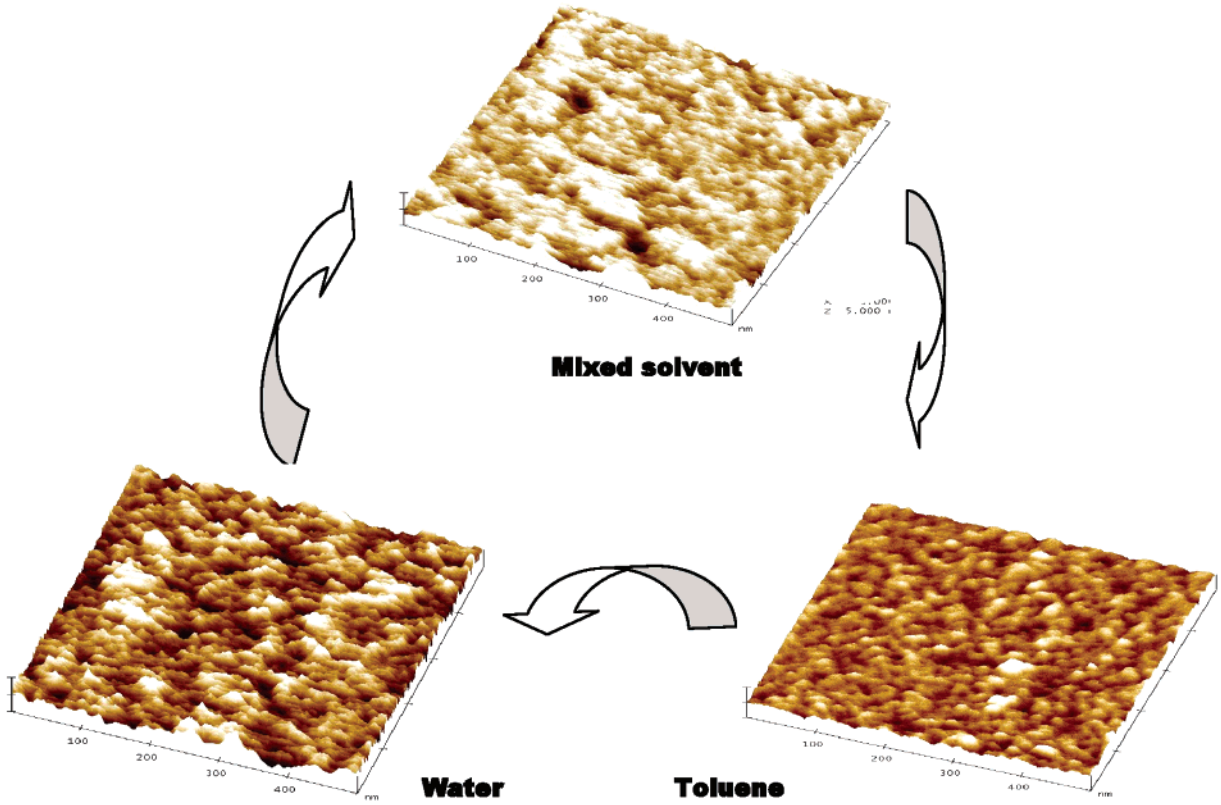

Figure 2. Representative 3D topographical images of **Y1** brush layer (500 nm × 500 nm × 10 nm) in different solvents.

air under an assumption of the identity of their "frozen-in" state to that occurring at a solid−fluid interface. To date, the actual surface morphology and properties of these responsive surfaces under fluids remain unknown.

Here, we report on the first *direct observation* of the nanoscale interfacial structures under different fluids (at solid-fluid interfaces) of Y-shaped brushes (see chemical formulas in Figure 1). We used solvents of different quality and evaluated brush nanoscale properties with surface force spectroscopy (elastic response and adhesive properties). The synthesis of the Y-shaped molecules presented in Figure 1 and the fabrication of chemically grafted layers followed by hydrolysis are described in detail elsewhere.[21,22] Atomic force microscopy (AFM) studies in the tapping mode were performed on a Multimode Nanoscope IIIa microscope equipped with a fluid cell according to the procedure adapted in our lab.[26] Probing of nanomechanical surface properties was conducted directly in fluids by surface force spectroscopy using cantilevers with known spring constants and tip radii.[27] Force volume mode within 300 nm × 300 nm surface areas was applied to collect 16 × 16 and 32 × 32 arrays of force−distance curves. The force−distance data processing and calculation of the elastic modulus and surface histograms were carried out in accordance with the Hertzian-based multilayered contact mechanics model. This model considers influence of the substrate on the elastic response and allows calculation of true elastic modulus as discussed elsewhere.[26−29]

AFM imaging of **Y1** and **Y2** brush layers in toluene (selective solvent for PS arms), water (selective solvent for PAA arms), and mixed solvent of chloroform and methanol (1:1) (good solvent for both arms) revealed surface morphology with grainy nanoscale texture (Figure 2). The average thickness of the brush layers determined from a scratch test in fluid was close to 6 nm in different solvents. This value was much higher than the effective thickness of 1.4 and 1.9 nm measured for **Y1** and **Y2** brush layers in a dry state.[23] This significant (4-fold) increase in thickness in selective solvents indicates the swelling of arms and the formation of truly brush-like structure with stretched chains as predicted for densely grafted polymer chains in brush regime.[22]

The surface microroughness reached 0.7 nm in water and 0.44 nm in toluene for **Y1** brush layer, and 1.6 nm in water and 0.26 nm in toluene for **Y2** brush layer as compared to the initial microroughness for functionalized silicon surface of <0.2 nm. The surface microroughness in water was consistently higher than in the dry state (0.7 vs 0.3 nm for **Y1** and 1.6 nm vs 0.3 nm for **Y2**).[22] This significant increase (more than two-fold) reflects a nonuniform molecular topography of the brush layers placed into a selective solvent. This phenomenon is caused by a vertical extension of PAA arms swollen in a good solvent with PS chains remaining in a collapsed state as demonstrated in Figure 3. On the other hand, the lower surface microroughness for both brush layers in toluene can be associated with swollen PS arms fully "screening" collapsed PAA arms (see arrangements in Figure 3). It is important to emphasize that the volume fraction of PS arms is nearly two times greater than that of PAA arms (0.66 vs 0.34). Finally, higher surface microroughness observed in the mixed solvent reflects concurrent swelling of both long-chain PS arms and short-chain PAA arms. Close inspection of high-resolution AFM images obtained for **Y1**

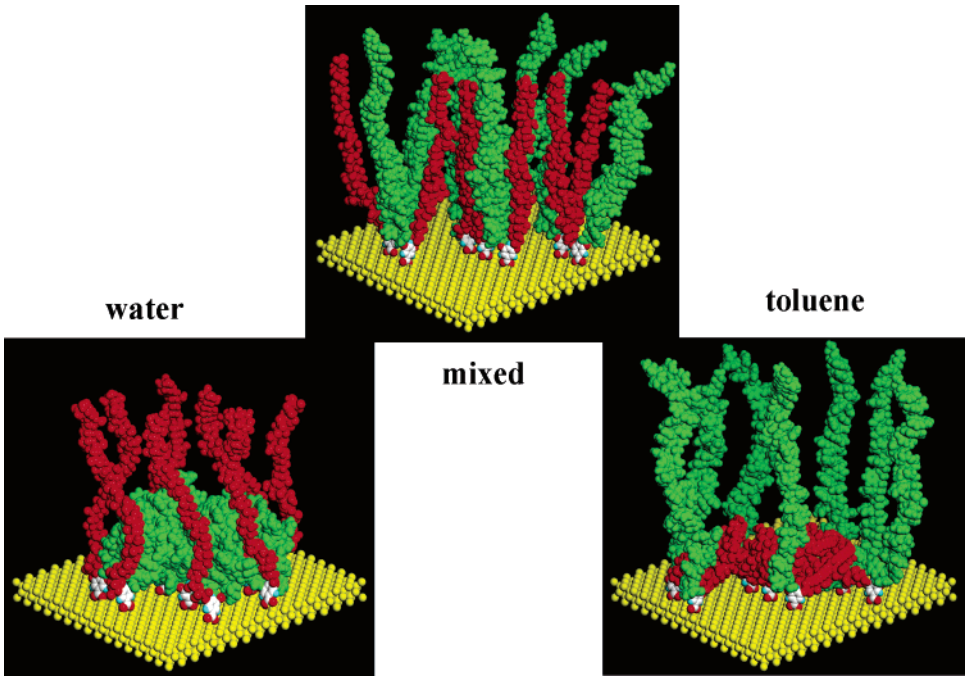

Figure 3. Molecular graphics showing internal molecular organization of an individual cluster comprising seven **Y1** molecules (green and red chains represent PS and PAA arms, respectively) in different solvents corresponding to the images in Figure 2.

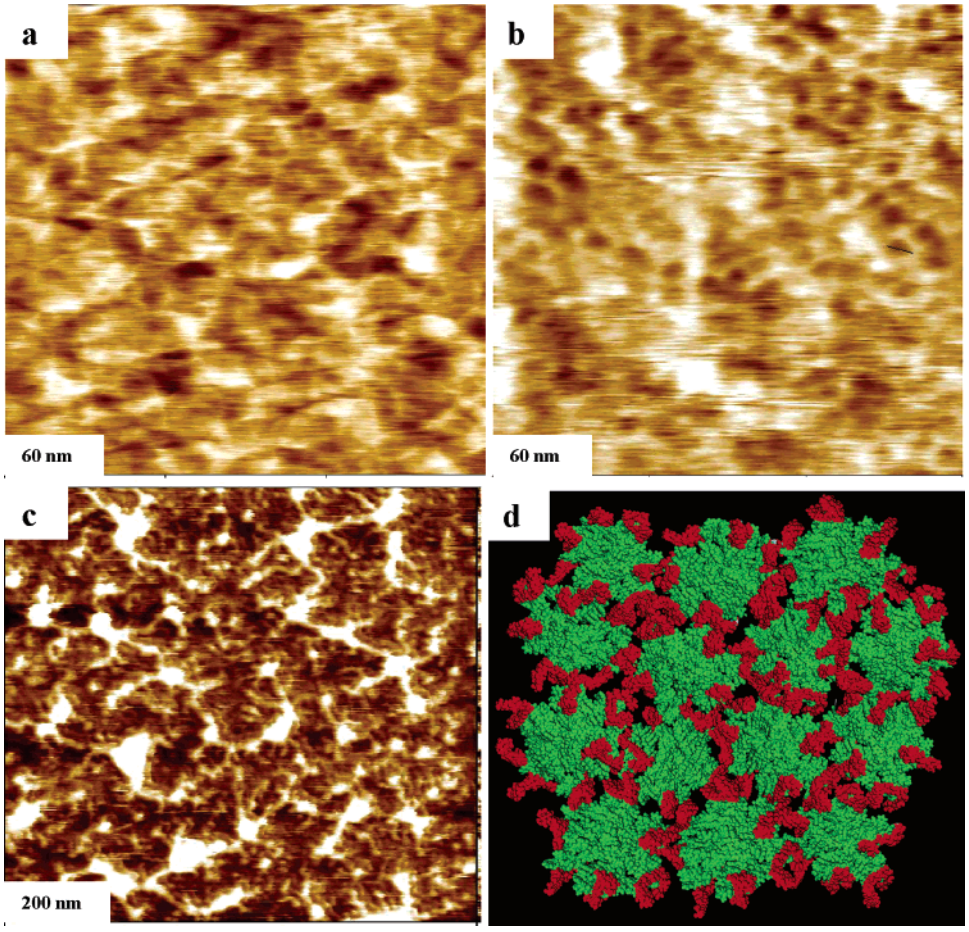

Figure 4. High-resolution AFM topographical images for **Y1** (a) and **Y2** (b) brush layers in water, **Y1** brush layer in dry state decorated with adsorbed gold nanoparticles (d), and corresponding molecular graphics of PS and PAA nanophases distribution within the layer (d).

brushes directly in different solvents revealed a random network of elevated ridges running across the surface (Figure 4a). This network is more ordered for **Y2** brush layer with occasionally seen local ordering expanding over a hundred

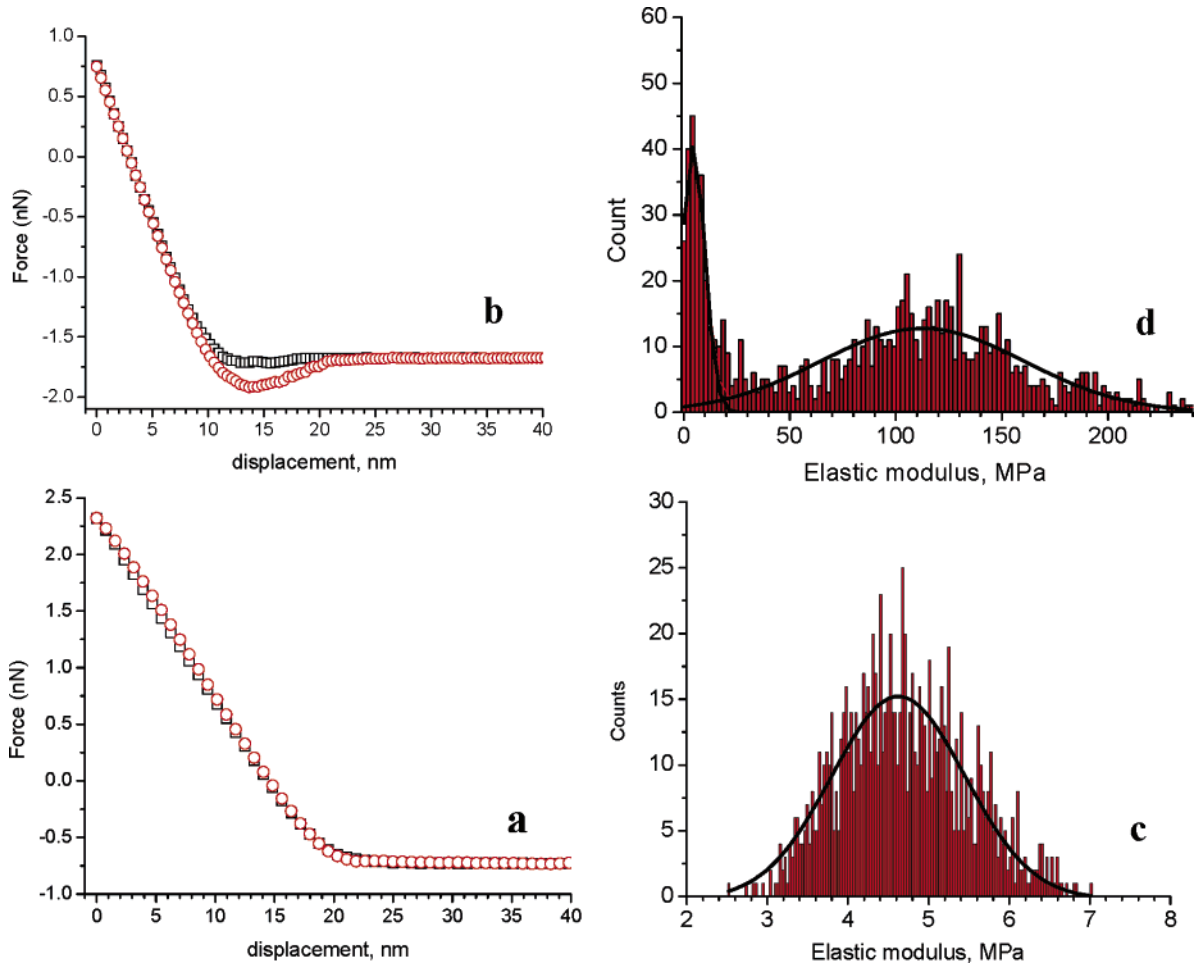

Figure 5. Results of nanomechanical probing of **Y1** brush layer in different solvents, toluene (a,c) and water (b,d): (a, b) representative force distance curves and (c,d) histograms of surface distribution of the elastic moduli. Squares are approaching cycles and circles are retracing cycles.

nanometers across and a cell dimension close to 20 nm (Figure 4b).

We suggest that this nanoscale topography is formed by extended PAA arms in water elevated above the nanosized mounds (∼15 nm) of collapsed PS chains. The PAA phase forms ridges separating PS mounds as represented schematically in Figure 4d. In this model, the red chains representing PAA arms elevated above collapsed PS domains composed of seven densely packed PS arms.[23] This molecular packing with the average cell size of 10−15 nm is close (but lower) to that observed experimentally. The PAA composition of these ridges is additionally confirmed by an independent study of adsorption of positively charged functionalized gold nanoparticles with a diameter of 5 nm (Figure 4c). In fact, we observed a strong preferential adsorption along the ridges with no nanoparticles adsorbed on flat areas of the brush layers. Apparently, such selective adsorption reflects neutral charge of PS-enriched surface areas and negatively charged PAA-rich ridges.

Weak nanoscale patterning observed directly in selective solvents has been predicted by the theoretical models for covalently grafted Y-shaped molecules.[19] The lateral dimension of network cells observed is controlled by the level of nanophase separation between PAA and PS arms attached to the same grafting points as depicted in the graphics representation (Figure 3). Finally, one should note that although the elements of the nanoscale patterning predicted by the theory can be observed, their in-fluid characterization remains very difficult because of a challenge of collecting high-resolution images of a swollen surface.

Significant changes in the surface properties (e.g., contact angle) were detected for the Y-shaped brush layers after treatment with different solvents in the dry state.[22,23] The in-situ surface reorganization under different fluids has never been explored before not only for Y-shaped brushes but for any other type of switchable layers as well.[30] Thus, we focused on the nanoscale properties of **Y1** brush layer (results for **Y2** layer are similar) by measuring the elastic response (the elastic modulus) and the adhesion (pull-off forces) directly in selective solvents, water and toluene (Figure 5).

Surface force spectroscopy confirmed the repulsive character of **Y1** brush layer in toluene with no adhesive loop observed for a retracing cycle (Figure 5a). This behavior is expected for weakly interacting surface such as a hydrophilic silicon tip and PS-enriched surface.[31,32] In stark contrast, significant adhesive forces were detected for the silicon tip interacting with the same Y-shaped brush in water. The pull-off forces reached 500 pN which is a high value expected

for strong interactions between the AFM tip with hydroxyl groups and a hydrophilic surface layer enriched with PAA arms.[31,32] Changes in adhesive forces measured directly in fluids are fully reversible and confirm the surface structural reorganization proposed for these Y-shaped brushes.[22]

The analysis of force−distance curves in accordance with a modified Hertzian model for multilayered surfaces[27] allowed us to evaluate the surface distribution of the elastic moduli, *E*, of brush layers in selective solvents (Figure 5c,d). Surface histograms measured directly in water with a lateral resolution below 10 nm showed bimodal distribution of the elastic response for Y-shaped brushes (Figure 5c). Compliant surface areas with low elastic modulus ($E = 4.3$ MPa) and stiffer surface areas with higher elastic modulus ($E = 110$ MPa) coexisted in water-swollen brush layer. Much lower elastic resistance is found on the surface areas occupied by PAA ridges. Both values of the elastic modulus were much lower than that estimated for the dry brush layer from similar nanomechanical mapping (430 MPa). The lower value of the elastic modulus is close to that observed for highly swollen polymers (e.g., polyelectrolytes in a good solvent).[33] However, even in this state, the collapsed but longer PS arms still occupy up to 35% of total surface in accordance with cluster models discussed earlier.[22] The presence of these surface areas combined with uncovered collapsed PS sublayer with higher elastic modulus causes bimodal elastic response.

In contrast, the testing of the elastic response of **Y1** brush layer in toluene which is a good solvent for PS arms showed a unimodal distribution of the elastic response with the average value of the elastic modulus centered around 4.6 MPa, a characteristic value for a polymer swollen in a good solvent (Figure 5d). These data indicate that the surface fraction of longer PS arms (vol. fraction 0.66) swollen in toluene is sufficient to completely cover the surface, thus, preventing the exposure of collapsed PAA arms. In addition, strong interaction between PAA chains and the hydrophilic silicon substrate may cause their uniform spreading in the immediate vicinity of the substrate.

In conclusion, direct, in-fluid observation of the surface morphology of binary brush layers composed of Y-shaped amphiphilic molecules revealed their grainy surface topography formed by coexisting stretched soluble arms in the brush regime and collapsed insoluble chains. Nanoscale patterning with short-range ordering was directly observed for the Y-shaped brush in water. Surface reorganization of Y-shaped brushes resulted in dramatic changes from repellent, compliant layer uniformly covered by swollen PS arms in toluene to an adhesive, mixed layer composed of coexisting swollen PAA and collapsed PS arms. The observed changes facilitate dramatic switching of macroscopic surface characteristics "frozen" in the post-treated, dry state leading to the controllable variation of the contact angle.[22] We believe that these binary surface layers with efficient switchable properties in different fluids and the overall thickness not exceeding several nanometers can serve as adaptive coatings for micro-nanofluidic channels with stimuli-responsive properties. The thickness of these switchable surface layers firmly grafted to the silicon surfaces is well below the thickness of conventional surface coatings (hundreds of nanometers) and that feature can be critical for controlling fluidic flow within channels with a diameter below 100 nm. The hydrophobic−hydrophilic contrast with nanoscale surface modulations may allow for size- and shape-selective nanoscale adsorption of various molecular species ranging from inorganic clusters to biological matter.

Acknowledgment. We acknowledge support by the National Science Foundation, CMS-0099868 and DMR-0308982 Grants. The authors thank M. Lemieux for fruitful discussions.

References

(1) Blossey, R. *Nat. Mater.* **2003**, *2*, 301.
(2) Nath, N.; Chilkoti, A. *Adv. Mater.* **2002**, *14*, 1243.
(3) Lafuma, A.; Quere, D. *Nat. Mater.* **2003**, *2*, 457.
(4) Jones, D. M.; Smith, J. R.; Huck, W. T. S.; Alexander, C. *Adv. Mater.* **2002**, *14*. 1130.
(5) Lahann, J.; Mitragotri, S.; Tran, T. N.; Kaido, H.; Sundaram, J.; Choi, I. S.; Hoffer, S.; Somorjai, G. A.; Langer, R. *Science* **2003**, *299*, 371.
(6) Luzinov, I.; Minko, S.; Tsukruk, V. V. *Prog. Polym. Sci.* **2004**, *29*, 635.
(7) Tsukruk, V. V. *Adv. Mater.* **2001**, *13*, 95.
(8) Ito, Y.; Ochiai, Y.; Park, Y. S.; Imanishi, Y. *J. Am. Chem. Soc.* **1997**, *119*, 1619.
(9) Mansky, P.; Liu, Y.; Huang, E.; Russell, T. P.; Hawker, C. *Science* **1997**, *275*, 1458.
(10) Ornatska, M.; Jones, S. E.; Naik, R. R.; Stone, M.; Tsukruk, V. V. *J. Am. Chem. Soc.* **2003**, *125*, 12722.
(11) Minko, S.; Muller, M.; Motornov, M.; Nitschke, M.; Grundke, K.; Stamm, M. *J. Am. Chem. Soc.* **2003**, *125*, 3896.
(12) Sidorenko, A.; Minko, S.; Schenk-Meuser, K.; Duschner, H.; Stamm, M. *Langmuir* **1999**, *15*, 8349.
(13) Zhao, B.; Brittain, W. J.; Zhou, W. S.; Cheng, S. Z. D. *J. Am. Chem. Soc.* **2000**, *122*, 2407.
(14) Ruths, M.; Johannsmann, D.; Ruhe, J.; Knoll, W. *Macromolecules* **2000**, *33*, 3860.
(15) Zhao, B.; Brittain, W. J. *Prog. Polym. Sci.* **2000**, *25*, 677.
(16) Müller, M. *Phys. Rev. E.* **2002**, *65*, 030802.
(17) Lemieux, M.; Usov, D.; Minko, S.; Stamm, M.; Shulha, H.; Tsukruk, V. V. *Macromolecules* **2003**, *36*, 7244.
(18) (a) Julthongpiput,D.; LeMieux, M.; Tsukruk, V. V. *Polymer* **2003**, *44*, 4557. (b) Lemieux, M.; Minko, S.; Usov, D.; Stamm, M.; Tsukruk, V. V. *Langmuir* **2003**, *19*, 6126.
(19) Balazs, A. C.; Singh, C.; Zhulina, E.; Gersappe, D. **1997**, *103*, 234.
(20) Zhulina, E.; Balazs, A. C. *Macromolecules* **1996**, *29*, 2667.
(21) Teng, J.; Zubarev, E. R. *J. Am. Chem. Soc.* **2003**, *125*, 11840.
(22) Julthongpiput, D.; Lin, Y. H.; Teng, J.; Zubarev, E. R.; Tsukruk, V. V. *Langmuir* **2003**, *19*, 7832.
(23) Julthongpiput, D.; Lin, Y. H.; Teng, J.; Zubarev, E. R.; Tsukruk, V. V. *J. Am. Chem. Soc.* **2003**, *125*, 15912.
(24) Zhao, B. *Polymer* **2003**, *44*, 4079.
(25) (a) Zhao, B.; Haasch, R. T.; MacLaren, S. *Polymer* **2004**, *45*, 7979. (b) Zhao, B.; Haasch, R. T.; MacLaren, S. *J. Am. Chem. Soc.* **2004**, *126*, 6124.
(26) Tsukruk, V. V. *Rubber Chem. Technol.* **1997**, *70*, 430.
(27) Kovalev, A.; Shulha, H.; Lemieux, M.; Myshkin, N.; Tsukruk, V. V. *J. Mater. Res.* **2004**, *19*, 716.
(28) Tsukruk, V. V.; Sidorenko, A.; Gorbunov, V. V.; Chizhik, S. A., *Langmuir* **2001**, *17*, 6715.
(29) Sidorenko, Ahn, A.; H.-S.; Kim, D.-I.; Yang, H.; Tsukruk V. V. *Wear* **2002**, *252*, 946.
(30) Advincula, R. C.; Brittain, W. J.; Caster, K. C.; Ruhe J. *Polymer Brushes*; Wiley: Weinheim, 2004.
(31) Noy, A.; Vezenov, D. V.; Lieber, C. M. *Annu. Rev. Mater. Sci.* **1997**, *27*, 381.
(32) Tsukruk, V. V.; Bliznyuk, V. N. *Langmuir* **1998**, *14*, 446.
(33) Vinogradova, O. I.; Andrienko, D.; Lulevich, V. V.; Nordschild, S.; Sukhorukov, G. B. *Macromolecules* **2004**, *37*, 1113.

NL0479029